Thermal Characteristics of a Vertical Guideway System including Hydrostatic Bearings and Ballscrew Drive of Precision Milling Machines

Hua-Chih Huang and Wen-Hao Yang

August 6, 2018

Thermal Characteristics of a Vertical Guideway System including Hydrostatic Bearings and Ballscrew Drive of Precision Milling Machines

Hua-Chih Huang*, *Wen-Hao* Yang

National Kaohsiung University of Science and Technology, Mechanical Engineering Department, 415 Chien-Kung Road, Sanmin District, Kaohsiung, 807 Taiwan

Abstract. This paper simulates the thermal characteristics of a vertical hydrostatic guideway using ANSYS/Fluent in precision milling machine applications by considering the oil film friction of hydrostatic bearings in operational feed speed and heat generation in ballscrew nut . Temperature rise in individual hydrostatic bearing due to different supply pressure, feed speed, and oil viscosity will be analyzed, and the thermal displacement of the center point of worktable can be predicted in case of thermal deformation.

Key words: thermal deformation, vertical hydrostatic guideway, finite element analysis

1 Introduction

A vertical guideway system consisting of hydrostatic bearings and ballscrew shown in Figure 1 will be the model of this study. The close-form design of hydrostatic guideway applied in a single rail is shown as Figure 2. The rectangular recess with depth of 1mm is chosen for the oil pocket design. For each bearing pad, the load carrying capacity $F = P_r \cdot A_e$, where P_r is the recess pressure, A_e is effective area of loading, and A_e= (L-a) ·(B-b). The design of hydrostatic bearings in worktable shown in Figure 3, and the dimensions of each bearing pad are shown in Figure 4 and Table 1.

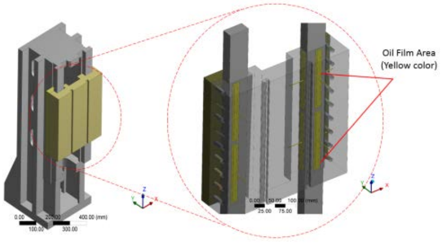

Fig. 1. Vertical hydrostatic guideway.

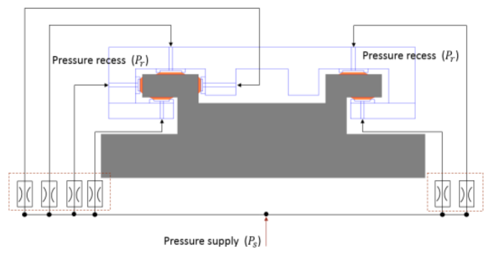

Fig. 2. Arrangement of hydrostatic bearings.

* Corresponding author: HC.Huang@nkust.edu.tw

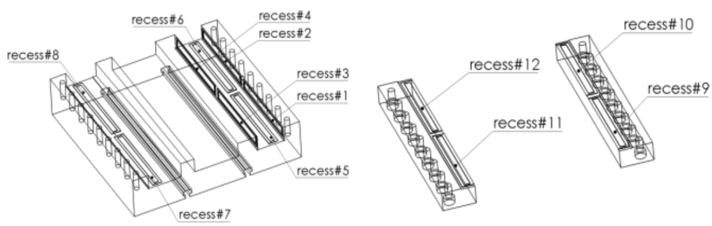

Fig. 3. Bearing pad design in worktable.

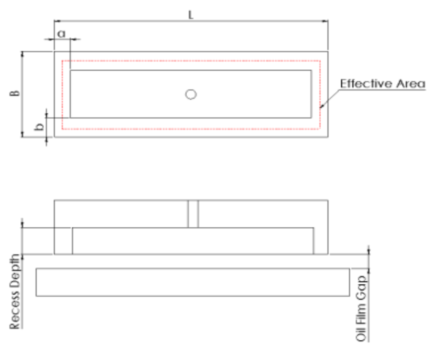

Fig. 4. Dimensions of bearing pad.

Table 1. Data of bearing dimensions

Dimension	Normal Recess	Side Recess
L(mm)	170	170
B(mm)	20	22
a(mm)	5	3.5
b(mm)	5	3.5
$A_e(mm^2)$	2475	3080.25
Film Clearance(μm)	10	10
Recess Depth(mm)	1	1

2 Methodology

The configuration of hydrostatic bearings considered in this paper is recess type hydrostatic bearing with a capillary-type restrictor(eg. Figure 5). The temperate rise (ΔT) of oil fluid is due to two contributions. Firstly it is the friction power (P_f) of oil film in a small gap, which relates to the feed speed, viscosity grade of the oil, oil film clearance and effective area of the bearing pad. Secondly, it is due to the pumping power (P_p) of the oil supply system [1].

$$P_f = \mu V^2 \left(\frac{A}{h}\right)$$

$$P_p = P_s \cdot Q_p$$

$$\Delta T = \frac{P_f + P_p}{c\rho Q_p}$$

Where μ is the viscosity of the oil (Pa · s), V is the sliding feed speed (m/s), A is the total area of bearing pads (m^2), h is the oil film clearance (m), P_s is the supply pressure of the oil (N/m^2), Q_p is the flow rate.

The thermal effect of the vertical guideway system comes from two main contributions: one is from the oil film sliding effect of hydrostatic bearings, and the other is from the friction heat of ballscrew nut. Thermal deformation of worktable resulting from ballscrew nut is shown in Figure 6.

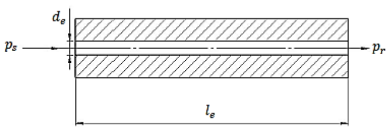

Fig. 5. Capillary restrictor

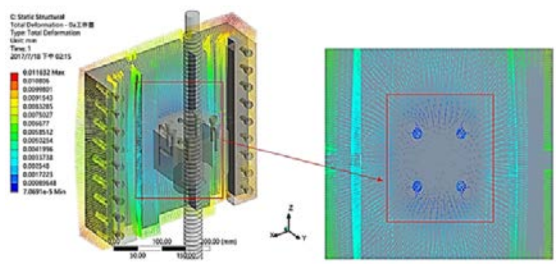

Fig. 6. Thermal deformation in ballscrew nut

3 Results and Discussions

The temperate rise in the vertical hydrostatic guideway will be analyzed with respect to different oil film clearance (10μm~30μm), sliding feed speed (0.1m/s~1m/s) by considering different supply pressure (10bar, 15bar, 20bar) and oil viscosity grade (VG46, VG32, VG15)[2,3,4]. Some selected results are shown in Figure 7 and 8. Note that the temperate rise happens mainly on the bearing sill due to the small film clearance.

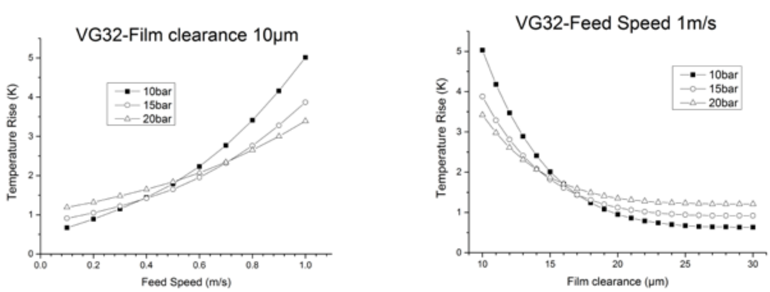

Fig. 7. Temperature rise w.r.t. supply pressure (VG32)

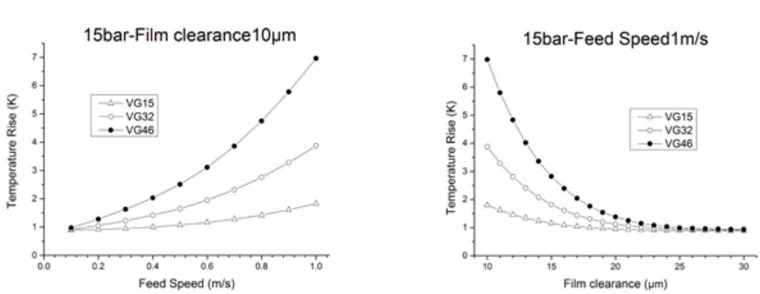

Fig. 8. Temperature rise w.r.t. viscosity grade (15 Bar)

Forces on the normal recess (2443N) and side recess (3049N) can be obtained from Ansys/Fluent analysis in Figure 9. Figure 10 shows the structural deformation of clamp plate in worktable due to recess pressure. The recess pressure acting on the fixed rail of the guideway system is illustrated in Figure 11, and its result indicates that of minor effect on the rail deformation(deformation of 0.076162µm only), therefore we ignore its effect in this study. The thermal deformation at fixed position of the ballscrew nut under the worktable is indicated in Figure 12. Thermal displacement of path line in the center worktable is shown in Figure 13. Figure 14 explains the shifting of worktable center point resulting from thermal deformation. The axial displacements of center point are shown in Table 2.

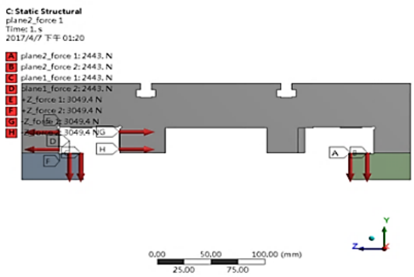

Fig. 9. Forces acting on the recess area

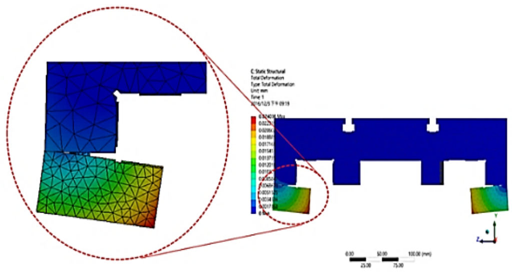

Fig. 10. Clamp plate deformed due to recess pressure

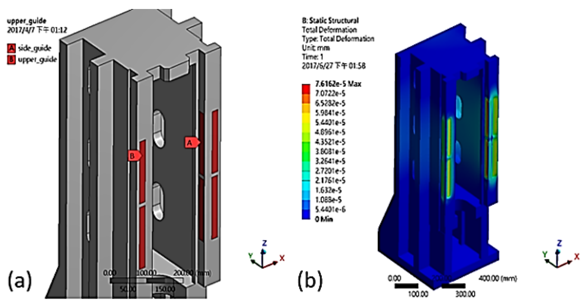

Fig. 11. (a)Recess pressure acting on fixed rail, (b) Structural deformation on fixed rail.

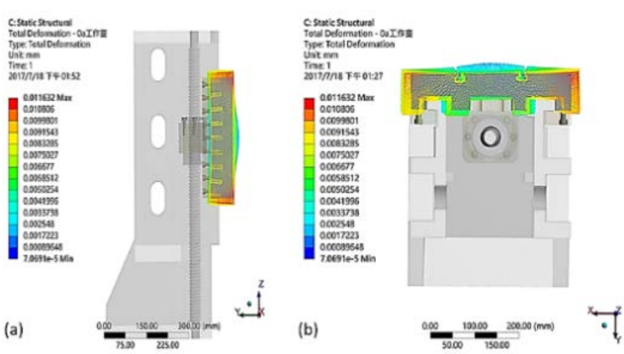

Fig. 12. Thermal deformation of the worktable.

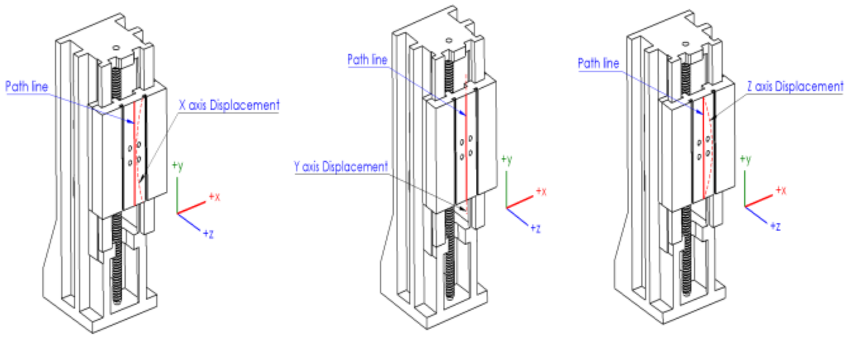

Fig. 13. Displacement of path line in X,Y, Z direction.

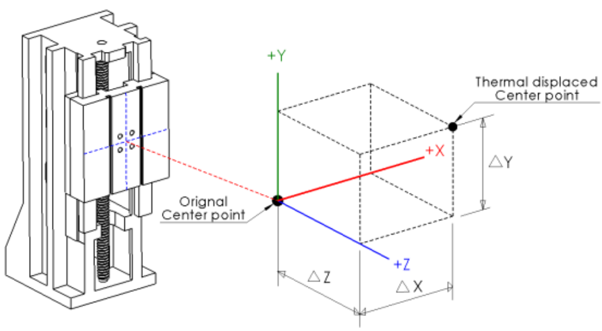

Fig. 14. Shifting of worktable center point resulting from thermal deformation

Table 2. Axial displacement of center point (worktable)

Axial displacement(μm)		
ΔX	ΔY	ΔZ
0.1539	0.0009	2.0246

4 Conclusions

The simulations of thermal characteristics of this vertical hydrostatic guideway conclude the following results:

(1) Load carrying capacity of hydrostatic bearing will be reduced 7.38% and 6.83% respectively, owing to the structural deformation of two clamp plates.

(2) Under the sliding feed speed of 1m/s, the positioning error of worktable center point is 0.1539μm in X direction, 0.0009μm in Y direction, and 2.0246μm in Z direction.

Acknowledgement :The financial support of this research from Ministry of Science and Technology of Taiwan (project no. MOST 106-2221-E-151-021) is gratefully acknowledged.

References

1. W. B. Rowe, Aerostatic and Hybrid Bearing Design, Butterworth-Heinemann, (2012).

2. Z. Wang, W. Zhao, B. Li, J. Zhang and B. Lu, Fluid-structure interactions (FSI) on static characteristics of hydrostatic guideways, *IEEE International Symposium on Assembly and Manufacturing (ISAM)*, 1-5, (Tampere, 2011).
3. S. Yang, P. Zhao, Y. Xu, I. Sun, P. Wu, X. Long and Z. Jiang, Hydrostatic Worktable Performance of an Ultra-precision Optical Aspheric Machine Tool, *Procedia CIRP*, 27, 187-191, (2015).
4. Z. Liu, C. Zhan, Q. Cheng, Y. Zhao, X. Li and Y. Wang, Thermal and tilt effects on bearing characteristics of hydrostatic oil pad in rotary table, *Journal of Hydrodynamics, Ser. B*, 28, 585-595, (2016).